

Analyst

Accepted Manuscript



This is an *Accepted Manuscript*, which has been through the Royal Society of Chemistry peer review process and has been accepted for publication.

Accepted Manuscripts are published online shortly after acceptance, before technical editing, formatting and proof reading. Using this free service, authors can make their results available to the community, in citable form, before we publish the edited article. We will replace this *Accepted Manuscript* with the edited and formatted *Advance Article* as soon as it is available.

You can find more information about *Accepted Manuscripts* in the [Information for Authors](#).

Please note that technical editing may introduce minor changes to the text and/or graphics, which may alter content. The journal's standard [Terms & Conditions](#) and the [Ethical guidelines](#) still apply. In no event shall the Royal Society of Chemistry be held responsible for any errors or omissions in this *Accepted Manuscript* or any consequences arising from the use of any information it contains.



Analyst

ARTICLE

Evaluation of Drift Gas Selection in Complex Sample Analyses Using a High Performance Drift Tube Ion Mobility-QTOF Mass Spectrometer

Received 00th January 20xx,
Accepted 00th January 20xx

DOI: 10.1039/x0xx00000x

www.rsc.org/

Ruwan. T. Kurulugama,^{*a} Ed Darland,^a Frank Kuhlmann,^a George Stafford^a and John Fjeldsted^a

A recently developed uniform-field high resolution ion mobility (IM) quadrupole time of flight (Q-TOF) mass spectrometer is used for evaluating the utility of alternate drift gases for complex sample analyses. This study provides collision cross section comparison for 275 total pesticides including structural isomers in nitrogen, helium, carbon dioxide, nitrous oxide and sulfur hexafluoride drift gases. Furthermore, a set of small molecules and Agilent tune mix compounds were used to study the trends in experimentally derived collision cross section values in argon and the alternate drift gases. Two isomeric trisaccharides, melezitose and raffinose, were used to evaluate the effect of the drift gasses for mobility separation. The hybrid ion mobility Q-TOF mass analyzer used in this study consists of a low pressure uniform field drift tube apparatus coupled to a high resolution Q-TOF mass spectrometer. Conventionally, low pressure ion mobility instruments are operated using helium drift gas to obtain optimal structural information and collision cross-section (CCS) values that compare to theoretical CCS values. The instrument employed in this study uses nitrogen as the standard drift gas but also allows the utility of alternate drift gases for improved structural analysis and selectivity under certain conditions. The use of alternate drift gases with a wide range of polarizabilities allows the evaluation of mobility separation power in terms of induced dipole interactions between the drift gas and the analyte ions.

Introduction

Ion mobility (IM) spectrometry, first popularized by Karasek, Mason and McDaniel in early 1970s as plasma chromatography, has become a valuable analytical technique for structural analysis and rapid separation of complex mixtures.^{1,2,3} The recent developments and present wide use of ion mobility in biological sample analysis is mainly due to efforts by the groups of Bowers, Jarrold and Clemmer.^{4,5,6,7} IM in complex sample analyses was demonstrated by Valentine et al. when they coupled liquid chromatographic techniques with high resolution ion mobility spectrometry and time-of-flight mass spectrometry for complex peptide mixture analyses.⁸ Structural analyses of gas phase ions was complemented by the development of theoretical methods for the calculation of collision cross section (CCS) values that can be compared with ion mobility experimentally derived CCS values.^{9,10,11} Early IM instruments used Bradbury-Nielsen ion gates for introducing ions into the drift tube.^{12,13} The very low duty cycle associated with this ion introduction method inhibited the use of ion mobility for high throughput complex sample analyses. However, with the

invention of the ion funnel technology by Smith's group, it became possible to trap and release ions at relatively high pressure allowing the development of highly sensitive IM mass spectrometry (MS) instrumentation.^{14,15} Recent developments in high resolution IM-MS technology can achieve mobility separations approaching and exceeding liquid chromatographic techniques.¹⁶ Owing to these technical advancements, ion mobility coupled to mass spectrometry has become a standard tool in the analytical toolbox. As more researchers gain access to IM-MS, new and more complex problems are probed and reported using the IM-MS technique. Thus it is invaluable to explore the use of alternate drift gases to facilitate the separation power of the IM instruments for both complex mixture analysis as well as in structural analysis.

Alternate Drift Gasses

Although early research ion mobility instruments primarily used helium as the drift gas, due to the focus on structural analysis, currently available commercial instruments use nitrogen as the standard drift gas. Nitrogen is favored due to cost and the high breakdown voltages that can be achieved. Although the performance of the IM system is similar using either nitrogen or helium, in some applications, such as the structural analysis of molecules, it is advantages to use helium as the drift gas. CCS values generated experimentally with IM using helium drift gas can be readily compared with theoretically calculated CCS values.⁹

^a Agilent Technologies, 5301 Stevens Creek Blvd. Santa Clara, CA, 95051, USA

E-Mail: ruwan_kurulugama@agilent.com

* Corresponding author

† Footnotes relating to the title and/or authors should appear here.

Electronic Supplementary Information (ESI) available: [details of any supplementary information available should be included here]. See

DOI: 10.1039/x0xx00000x

With the commercial availability of uniform field and travelling wave IM-MS instruments, it is more valuable to evaluate the use of alternate drift gases for specific purposes such as improving separation and selectivity. Several research groups have employed alternate drift gases and studied the effect of the drift gases for mobility separation.^{17,18,19,20} The CCS for a given ion is a function of the size of the analyte ion, size of the drift gas molecule, and the chemical and physical nature of the interactions between the analyte ions and the drift gas. Therefore, the CCS values for a given ion varies with the size and the polarizability of the drift gas. The variation in the CCS values with different drift gases has been studied using drift tube-MS and differential mobility analysis-MS techniques in combination with density functional theory (DFT) calculations and molecular dynamic simulations.^{21,22,23} Hill and co-workers found that for a set of small metabolites and peptides CCS values increased linearly with the polarizability of the drift gas.²⁴

Molecular Separation

The basis of separation in IM is primarily due to the size and charge state of the ion and to a lesser extent the nature of the drift gas. Therefore, in theory, separation and selectivity in IM can be altered by using different drift gases, using different adducts or reagents, and changing structure of ions by collisional activation.²⁵ Ruotolo et al. found that ion mobility peak capacities were similar for a mixture of tryptic peptides using He, N₂, Ar, and CH₄ drift gases, but at the same time they observed that some peptides were selectively separated based on their structure and the drift gas.²⁰ Creaser and co-workers used polyethylene glycols (PEG) and crown ethers as shift reagents to improve ion mobility separation of pharmaceuticals and protonated amines, respectively.²⁶ Bohrer et al. have used a similar techniques to improve the separation of peptide mixtures using crown ethers.²⁷ Although high resolution IM instruments can separate structural isomers, the separation of optical isomers using ion mobility is much more difficult. In research by Dwivedi et al., chiral compounds were separated by doping the chiral modifier (*S*)-(+)-2-butanol into the nitrogen drift gas in a technique referred to as chiral ion mobility spectrometry (CIMS).²⁸ CIMS was shown to be able to separate several small chiral compounds from racemic mixtures using an atmospheric pressure drift tube IM instrument.

IM-MS has become a useful analytical tool for analyzing complex samples in fields such as metabolomics, proteomics, glycomics and lipidomics. The present study includes the separation of a large number of pesticides using high performance liquid chromatography followed by ion mobility separation and mass spectrometry analysis. CCS values for pesticides with proton, sodium, potassium, and ammonium adducts were derived using He, N₂, CO₂, and N₂O drift gases. In this study we have also generated CCS values for a variety of small molecules, consisting of natural products, medicines and pesticides identified in different drift gases. The CCS libraries generated in this study can be subsequently used for pesticide analysis in complex matrices.

Experimental

IM Q-TOF Instrumentation

In an IM instrument ions are separated as they pass through the ion mobility cell based on their size and charge.²⁹ Ions with larger collision cross sections undergo a greater number of collisions with drift gas molecules compared to ions with smaller collision cross sections. Therefore, larger ions travel through the drift cell slower than smaller ions. Additionally, ions with higher charge states experience a greater electric force resulting in greater velocities compared to ions of the same collision cross section but with a lower charge state. The drift cell is typically operated under low-field limit conditions allowing the instrument to generate accurate structural information for compounds.³ Under low electric field conditions ion mobility is not dependent on the electric field but rather on structure of the molecule and interaction with the drift gas. The average velocity (v_d) of ions in a drift cell is given by equation (1)

$$\overline{v_d} = KE \quad (1)$$

where E is the electric field and K is the proportionality constant known as mobility.

An expression for reduced mobility (K_0), which is normalized to pressure and temperature, is given by equation (2). Reduced mobility can be used to identify compounds because it is only a function of the structure of the compound and the drift gas used and is not dependent on the instrument or the instrumental conditions used

$$K_0 = \frac{L}{t_d E} \frac{P}{760} \frac{273.2}{T} \quad (2)$$

where L is the length of the drift cell, t_d is the corrected drift time, E is the electric field across the drift cell, P is the pressure of the drift cell and T is the temperature of the drift gas.

All of the experiments were carried out using a commercially available Agilent 6560 IM Q-TOF instrument with the optional alternate drift gas kit installed (Agilent Technologies, Santa Clara, CA). Figure 1 shows a schematic of the Agilent IM Q-TOF

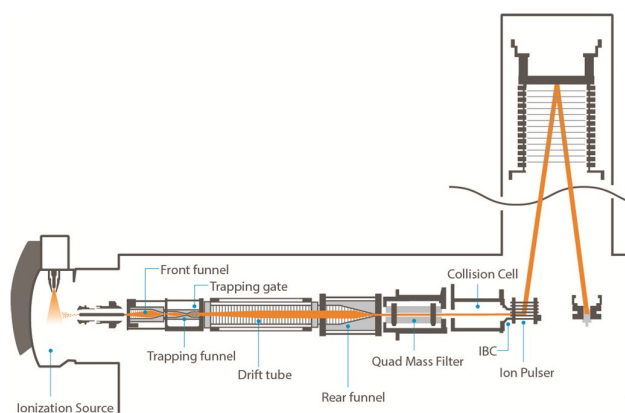


Figure 1. Schematic diagram of the ion mobility Q-TOF instrument. Ions generated in the source region are carried into the front ion funnel through a single-bore glass capillary. The trapping funnel accumulates and release ions into the IM drift tube. Ions are separated in the ~78 cm long drift cell which is typically operated at a ~18 V/cm drift field. Ions exiting the drift tube enter the rear ion funnel which compresses the ion beam before transmission to the high resolution Q-TOF mass analyzer.

instrument with the ion optics elements between the IM apparatus and the Q-TOF system omitted for simplicity. The IM Q-TOF system consists of a front ion funnel, trapping ion funnel, drift tube, and a rear ion funnel that couples through a hexapole ion guide to the quadrupole time-of-flight mass analyzer. The front ion funnel was operated at 4.8 Torr with ~ 15.0 V/cm DC electric field and 120 V_{p-p} (peak-to-peak) RF electric field at 1.4 MHz. The trapping ion funnel was operated at 3.71 to 3.80 Torr, depending on the drift gas used, and ~ 18.0 V/cm DC electric field and 120 V_{p-p} RF electric field at 1.1 MHz. The drift cell consists of 175 ring electrodes (~ 78 cm long) with a 5 cm inner diameter and is manufactured using printed circuit boards and coated with gold. The drift tube was operated at 3.94 Torr and 8.3 V/cm DC electric field for helium drift gas and 17.3 V/cm for all other drift gases, unless stated otherwise. This instrument is equipped with a thermocouple gauge inside the drift tube for accurate temperature measurement but does not allow active temperature regulation. The typical drift tube temperature is 300 K. The rear ion funnel was operated at same pressure as the drift tube and used ~ 17.0 V/cm DC electric field and 150 V_{p-p} RF electric field at 1.2 MHz. The hexapole ion guide, which couples the IM apparatus and Q-TOF, was operated at 8 V potential difference. The collision cell and ion beam compressor were operated with a 9 and 3 V DC potential difference, respectively.

The experiments were carried out using an electrospray ionization source (Agilent Jet Stream-ESI). This is an electrospray ionization source with a thermal gradient focusing technology. This source uses a nebulizer gas and a super heated sheath gas to improve the desolvation and gas phase ion generation. The Agilent Jet Stream ion source was operated in the positive ion mode.

The alternate drift gas kit installed on this instrument allowed the use of drift gases other than nitrogen. This kit consists of two capacitance diaphragm gauges (CDG) for pressure measurement, an electronic pressure regulator and controller electronics. Gas-type independent, true pressure measurements can be obtained using a CDG. CDG pressure gauges also have a high accuracy rating and a reproducibility specification of $<0.2\%$. The electronic pressure regulator maintains the gas pressure in the drift tube by monitoring the signal from the CDG attached to the drift tube and adjusting the upstream pressure in the trapping funnel by controlling the amount of gas introduced into the trapping funnel. The alternate gas kit can maintain the drift tube pressure within ± 5 mTorr from the setpoint. The pressure difference between the trapping funnel and the drift tube was adjusted such that drift tube pressure was always higher than the trapping funnel pressure to obtain maximum gas purity within the drift tube. For nitrogen drift gas experiments, the pressure difference was maintained at 150 mTorr, while for helium the pressure difference was 230 mTorr. For all of the other gases the pressure difference was maintained at 210 mTorr.

The ion mobility Q-TOF instrument was operated in extended dynamic range mode with a 1700 m/z range. The scan rate was set to 1.5 frames per second. The ion funnel trap was operated at varying trap fill time settings to obtain the optimum system sensitivity. Helium drift gas provided the best signal

intensities; the trap fill time setting of ~ 10 ms was shorter for helium than for experiments using other gases. The experiments with sulfur hexafluoride had the lowest signal intensities and required longer trap fill times to maintain reasonable signal intensities. Nitrogen, carbon dioxide, and nitrous oxide drift gas experiments yielded similar signal intensities. The trap release time for the experiments was 150 μ s, except for sulfur hexafluoride drift gas based experiments where 250 μ s was used, unless stated otherwise. Maximum drift time settings were also adjusted depending on the drift time shifts in different drift gases. For helium drift gas experiments, 30 ms maximum drift time was used while for nitrogen, carbon dioxide, nitrous oxide and sulfur hexafluoride drift gases, 40, 60, 60 and 105 ms maximum drift times were used, respectively.

Sample Preparation

Three sets of sample classes referred to as small molecules, tune mix, and pesticides were prepared and analyzed.

Small molecules. A variety of natural products and medicines were prepared to represent a wide mass range of small molecules (m/z 250 - 609). Alprenolol (m/z 250), ondansetron (m/z 294), clozapine N-oxide (m/z 343), colchicine (m/z 400), verapamil (m/z 455), and reserpine (m/z 609) were purchased from Sigma-Aldrich (St. Louis, MO). Samples were prepared at 0.01 mg/ml in a solution of water:acetonitrile 50:50% (v/v) with 0.1% formic acid. Melezitose and raffinose samples were purchased from Sigma-Aldrich (St. Louis, MO) and electrospray samples were prepared at 0.01 mg/ml in a solution of water:acetonitrile 50:50% (v/v) with 5.0 mM NaCl.

Tune mix. Agilent tune mix solution (m/z 322 - 1522, low concentration) was purchased from Agilent Technologies (Santa Clara, CA) and diluted 1:10 using a water:acetonitrile 5:95% (v/v) solution.

Pesticides. Eight pesticide mixtures containing 275 total pesticides, including isomers, at 100 ppm concentration were purchased from Agilent Technologies (Santa Clara, CA - Agilent comprehensive pesticide mixture). The pesticide stock solutions were diluted using water:methanol 70:30% (v/v) to obtain 100 ppb samples.

All reagents and solvents were HPLC grade. Acetonitrile and methanol were purchased from Honeywell (Morristown, NJ). Ultrapure water was produced using a Milli-Q Integral system equipped with a LC-Pak Polisher and a 0.22 μ m point-of-use membrane filter cartridge (EMD Millipore, Billerica, MA). Formic acid was purchased from Fluka (Sigma-Aldrich Corp., St. Louis, MO) and ammonium formate solution (5 M) was purchased from Agilent Technologies (Santa Clara, CA).

Liquid Chromatography

Separation was carried out using an Agilent 1290 Infinity II series UHPLC system (Santa Clara, CA) consisting of an Agilent 1290 Infinity Binary Pump with standard flow, an Agilent 1290 Infinity High Performance Autosampler, a sample cooler, and an Agilent 1290 Infinity Thermostatted Column compartment. A Rapid Resolution High Definition ZORBAX (RRHD) column with 2.1 x 150 mm dimensions and 1.8 micron particle size was used.

The LC flow rate was 400 $\mu\text{L}/\text{min}$. Mobile phase solutions were 100% water with 0.1% formic acid and 5 mM ammonium formate as solvent A and 100% MeOH with 0.1% formic acid and 5 mM ammonium formate as solvent B. A gradient elution method was used where solvent B is ramped from 5% to 10% in 0.5 min., then increased to 40% from 0.5-3.5 min., then further increased to 98% from 3.5-18.0 min., maintained at 98% for 2 min. and then finally decreased to 5% and maintained for an additional 5 min. for column re-equilibration. Triplicate runs were made with 1 μL injection of the 100 ppb pesticide samples. The LC column temperature was maintained at 40 $^{\circ}\text{C}$. LC experiments for pesticide samples were carried out in both Q-TOF only mode and IM mode of operation for nitrogen drift gas. For all other drift gases, only IM mode data were collected.

Data Analysis, CCS calculations and IM-MS Browser

Direct infusion experiments were performed using single electric field (8.3 V/cm for helium and 17.3 V/cm for all other drift gases, unless stated otherwise) and multiple electric fields for the same experiment with different time segments. Multiple electric fields experiments consisted of 0.5 min. time segments, each with a predetermined electric field for the drift tube. Depending on the drift gas used the multiple electric field method was modified to have a different set of electric field values. This multiple electric field method consisted of five time segments with 3.20, 3.85, 4.49, 5.13, and 5.77 V/cm for He experiments, 13.46, 14.75, 16.03, 17.31, and 18.59 V/cm for SF_6 experiments and 12.18, 13.46, 14.75, 16.03, and 17.31 V/cm for all other drift gases. Results from the multiple drift field experiments were used to calculate CCS values using a conventional method where instrument measured drift time was plotted against the inverse drift potential to obtain the t_0 value. The t_0 value corresponds to the time required for an ion to travel the distance between the exit of the drift tube and mass analyzer. The corrected drift time (t_d) is then calculated using equation (3)

$$t_d = t_D - t_0 \quad (3)$$

where t_D is the instrument measured drift time. The Mason-Schamp equation (4) uses the corrected drift times (t_d) to calculate the CCS values, and can be described as the classical multi-electric field method for CCS calculation,^{30,31}

$$\Omega = \frac{(18\pi)^{1/2}}{16} \frac{ze}{(k_b T)^{1/2}} \left[\frac{1}{m_i} + \frac{1}{m_B} \right]^{1/2} \frac{t_d E}{L} \frac{760}{P} \frac{T}{273.2} \frac{1}{N} \quad (4)$$

where Ω is the momentum transfer collision integral (the measured CCS value in this study), k_b is the Boltzmann constant, m_i and m_B are mass of the ion and drift gas, respectively, z , e , and T are ion charge state, elementary charge and temperature in kelvin respectively. E , L and P are electric field, length of the drift tube and pressure of the drift gas, respectively, and N is the number density of the drift gas. CCS values for LC separated pesticides were calculated using a calibration curve where the CCS values for the Agilent tune mix compounds (m/z 322 - 1522) in each drift gas were used as drift time calibrants as described previously.³² Briefly, instrument measured drift times (t_D) for any given ion consists of three related contributions from inside and outside the drift cell as given in equation (5)

$$t_D = t_{d(\text{inside})} + t_{d(\text{outside})} + t_{fix} \quad (5)$$

where t_D is the instrument measured drift time, $t_{d(\text{inside})}$ and $t_{d(\text{outside})}$ are mobility dependant drift times inside and outside the drift tube, respectively, and t_{fix} is a mobility independent flight time outside the drift cell. Substituting Mason-Schamp equation (4) into equation (5) and rearranging results in equation (6)

$$t_D = \beta \gamma \Omega + t_{fix} \quad (6)$$

where t_D , β , γ , Ω and t_{fix} are the instrument measured drift time, instrument dependent proportionality coefficient ($\text{ms}/\text{\AA}^2$), modified reduced mass related coefficient (unitless), collision cross section (\AA^2), and mobility independent flight time (ms), respectively. β is an empirically determined coefficient that is related to gas pressure, electric field, and geometry of the drift cell and other ion optics. The modified reduced mass related coefficient, γ , accounts for the charge of the ion (q) as shown in equation (7)³²

$$\gamma = \frac{1}{z} \sqrt{\frac{m_i}{m_i + m_B}} \quad (7)$$

where z is the ion charge state and m_i and m_B are mass of the ion and drift gas, respectively.

Plots of the instrument measured drift time (t_D) versus $\gamma\Omega$ for a set of tune mix compounds with known CCS values for the corresponding drift gas, under the same instrumental condition as the LC experiment, were used for obtaining β and t_{fix} coefficients for each drift gas used. These coefficients were used in calculating CCS values for each pesticide. The classical multi-electric field CCS calculation method was used to obtain the CCS values for the tune mix compounds in different drift gases. The calibration plots were generated using data obtained from direct infusion of the tune mix solution before and after the LC experiments for each drift gas.

Retention times for all of the compounds in the eight pesticide sub mixtures were determined using the LC-MS data with nitrogen drift gas. The retention time extraction was facilitated using the Find by Formula algorithm in Agilent MassHunter Qualitative Analysis. Drift times for the molecular ions for each of the pesticides were measured in the LC-IM-MS data with the aid of a custom software extension to the Agilent IM-MS Browser. The added software uses the known accurate mass and retention time of each compound to locate the corresponding molecular ion (or ions in the case of isomers). Once the drift times for each ion used were determined, the IM-MS Browser automatically calculates the corresponding CCS values using the method described above.

Results and Discussion

Small Molecules and Tune Mix Compounds

As shown in Figure 2A, CCS values for the Agilent tune mix compounds and the small molecules linearly scale with the size and the polarizability of the of the drift gas used. CCS values for the ions studied in helium are the smallest and in SF_6 are the largest. Two trend lines were observed for each gas, one for the tune mix compounds, shown in black dashed line, and one for the small molecules, shown in red dashed line. This indicates the

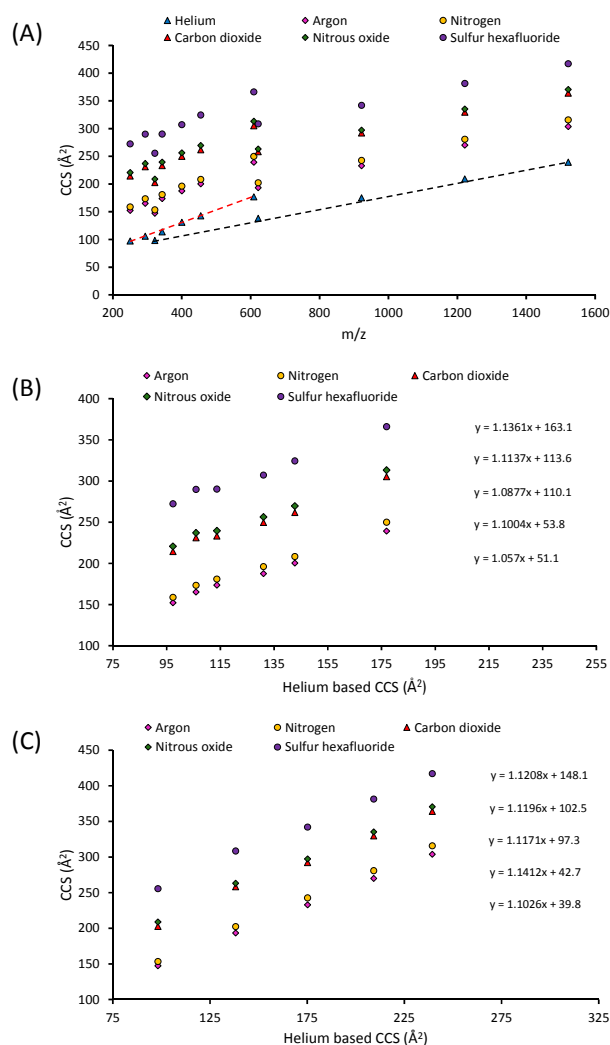


Figure 2. (A) CCS measurements for methoxyphosphazine and fluoro-phosphazine compounds from the Agilent tune mix and the small molecules (alprenolol, ondansetron, clozapine N-oxide, colchicine, verapamil and reserpine) in different drift gases. The CCS values for a give ion in different drift gases scale with the size of the drift gas atom or molecule and the polarizability of the drift gas used. (B) Correlation plots for CCS values between argon, nitrogen, carbon dioxide, nitrous oxide and sulfur hexafluoride drift gases versus helium drift gas for the small molecules (*m/z* 250 - 609). (C) Correlation plots for CCS values between argon, nitrogen, carbon dioxide, nitrous oxide and sulfur hexafluoride drift gases versus helium drift gas for the tune mix compounds (*m/z* 322 - 1522).

ability to separate different classes of molecules using ion mobility technology.^{16,33} The data were fitted to a power regression line ($y = Ax^B$) to obtain an equation to describe the correlation between the CCS value and *m/z*. For helium, the regression coefficients for the trend line corresponding to the small molecules are $A = 2.1807$ and $B = 0.6834$, while the regression coefficients for the trend line corresponding to the tune mix compounds are $A = 3.4841$ and $B = 0.5755$. The coefficient of determination (R^2) for the small molecules and the tune mix compound regression lines are 0.9912 and 0.9980, respectively.

The CCS trend lines indicate that different classes of molecules change size and shape differently with increasing

number of monomer units or increasing mass. Most of the tune mix compounds have a six membered hetero atom ring structure containing nitrogen and phosphorus atoms and side chains with increasing number of CHF₂ groups. Since the tune mix compounds have a different structure than the small molecule compounds used in this study, the CCS values for the two classes of compounds vary differently with increasing mass resulting in different trend lines and different correlation coefficients.

Evaluating the relative shift of CCS values in different drift gases can indicate molecular class. The average ratios between CCS values for the small molecules listed above in Ar, N₂, CO₂, N₂O, and SF₆ drift gases versus He drift gas are 1.46, 1.52, 1.92, 2.00, and 2.41, respectively. The average ratios between CCS values for Agilent tune mix compounds in Ar, N₂, CO₂, N₂O, and SF₆ drift gases versus helium drift gas are 1.33, 1.39, 1.68, 1.72, and 1.98, respectively. This indicates that the average relative shift of CCS values in different drift gases is somewhat dependent on the molecular class.

Collision cross section for a given ion is a function of the size of the ion, size of the drift gas, and the chemical and physical nature of the analyte ion and the drift gas interactions. As described by Larriba et al., the ion mobility is a measure of the drag force experienced by the ion when the system is at a thermal equilibrium, the ion motion is at or near the thermal velocity (low field limits), and the mean free path is relatively large compared to the ion size.^{21,22} Under the low field limits condition, CCS values can be directly calculated using the Mason-Schamp equation (4) and ion mobility measurement together with the charge state and mass of the ion and the mass of the drift gas. Based on extensive comparison of experimental and theoretical data using He and N₂ drift gases, Larriba et al. have determined that the CCS value for large ions primarily depends on the size of the ion and the drift gas and ion-induced dipole interactions have minor effects.²¹ In addition to this, the CCS value also depends on the inelastic diffused scattering of gas molecules during ion-neutral interactions, multiple gas molecule scattering where the same gas molecule interacts with the ion multiple times during a single interaction event, and both long range and short range ion-induced dipole potential interaction.

The average CCS for compounds shown in Figure 2 in Ar and N₂ drift gases indicates that both size of the drift gas and the nature of the ion-neutral interactions are responsible for observed CCS. The ratios of CCS between Ar/He and N₂/He for small molecule and tune mix compounds are 1.46, 1.52 and 1.33 and 1.39, respectively. However, the average van der Waals radius for Ar and N₂ are 1.88 Å and 1.55 Å, respectively; therefore, if the drift gas size is the only contributor for the value of the CCS then the Ar/He ratio should be larger than the N₂/He values.³⁴ Kim et al. have previously concluded that the contribution of the long range ion-neutral interaction contribution to CCS is about 30% for small ions and decreases to about 10% for larger ions of tertiary and quaternary ammonium cations using an atmospheric pressure drift tube ion mobility instrument and theoretical calculations.³⁵

In general the relative CCS shifts for most of the compounds are not far from the trend lines expected for each drift gas. Close inspection of the R^2 values for the regression lines among the different drift gases for the small molecules indicate that the CCS values for some molecules do not always shift by the same magnitude compared to other molecules in the same class. For example, clozapine N-oxide CCS values in different drift gases change differently from the average trend lines for the corresponding drift gases. The ratios between CCS values for clozapine N-oxide in Ar, N₂, CO₂, N₂O, and SF₆ drift gases versus He drift gas are 1.53, 1.59, 2.05, 2.11, and 2.55, respectively. This indicates that certain molecules can be selectively separated from some other molecules based on the drift gas used due to the enhanced induced-dipole interaction between the drift gas and the analyte ion, or lack thereof.

Figure 2B shows correlation plots for CCS values between Ar, N₂, CO₂, N₂O, and SF₆ versus He drift gas for alprenolol, ondansetron, clozapine N-oxide, colchicine, verapamil and reserpine. Based on the regression coefficients, on average a 51.1 Å² shift in CCS value is observed for Ar drift gas compared to He drift gas which correspond to a larger extent the contribution of the drift gas size for the observed CCS. On average 53.8, 110.1, 113.6 and 163.1 Å² shifts in CCS values are observed for N₂, CO₂, N₂O, and SF₆, respectively. However, the absolute average CCS increase compared to the He drift gas are 58.0, 66.8, 119.6, 125.9, and 175.2 Å² for Ar, N₂, CO₂, N₂O, and SF₆, respectively which correspond to the cumulative contributions from the drift gas size and the nature of the ion-neutral interaction. The He-N₂ CCS difference observed for these data agree well with the data published by May et al. for a large number of compounds with different chemical classes.³⁶

Figure 2C shows correlation plots for CCS values between Ar, N₂, CO₂, N₂O, and SF₆ versus He drift gas for tune mix compounds (m/z 322 - 1522). Based on the regression coefficients for this plot, on average 39.8, 42.7, 97.3, 102.5 and 148.1 Å² shifts in CCS values are observed for Ar, N₂, CO₂, N₂O, and SF₆ drift gases, respectively. The slope for most of the regression lines are in the order of 1.1 indicating that the shift in CCS for larger m/z ions are relatively higher compared to smaller m/z ions.

Resolving Power and Structural Isomer Separation

The instrument resolving power for the ion mobility separation is dependent on the initial pulse width, diffusional peak broadening, and the space charge related peak broadening.^{3,37} However, the resolving power for a given ion is also dependent on the structural rigidity of the ion. If an ion can change its three-dimensional structure during travel through the drift cell, such as an ion that can exist as different conformers with differing three-dimensional structures in the gas phase, it is not structurally rigid.³⁸ Ions with rigid structures and with a single conformer can be separated with the highest resolving power that can be achieved by the instrument configuration and the operating conditions. The diffusion limited resolving power for uniform field ion mobility instruments, which assumes infinitesimal initial ion packet peak

width and negligible space charge related peak broadening, is given by equation (8)³

$$R_D = \frac{t_d}{\Delta t} = \sqrt{\frac{LEQ}{16k_B T \ln 2}} \quad (8)$$

where t_d is corrected drift time, Δt is the full width at half-maximum (FWHM) of the drift peak, and L, E, Q are length of the drift tube, electric field across the drift cell and the ion charge, respectively. k_B and T correspond to Boltzmann constant and drift gas temperature, respectively. The resolving power is related to diffusion coefficient (D) through the Nernst-Einstein equation (9)

$$D = \frac{k_B T}{ze} K \quad (9)$$

where k_B, T, z, e and K are the Boltzmann constant, temperature, ion charge state, elementary charge and mobility of the ion, respectively. Equation (9) indicates that higher mobility ions result in higher diffusion. However, since ions with different mobilities arrive at the detector at different times, they have similar spatial peak widths and therefore similar

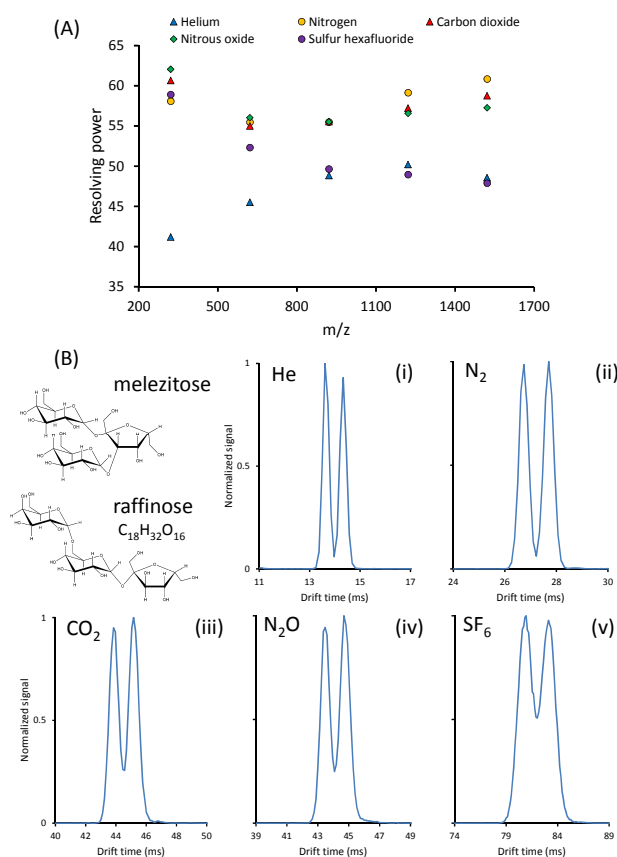


Figure 3. (A) Resolving powers for five Agilent tune mix compounds (m/z 322 - 1522) in nitrogen, helium, carbon dioxide, nitrous oxide and sulfur hexafluoride drift gases. Nitrogen, carbon dioxide and nitrous oxide drift gases produced similar drift resolution values for all compounds across the m/z range. Sulfur hexafluoride produced similar resolving power values to helium drift gas except for hexamethoxyphosphazine (m/z 322) and hexakis(2,2-difluoroethoxy)phosphazine (m/z 622). (B) Drift separation profiles for isomeric trisaccharides, melezitose and raffinose in a mixture as sodium adducts using different drift gases. For helium drift gas the drift tube was operated at 8.3 V/cm and for all the other drift gases 17.3 V/cm. The pressure in the drift tube was maintained at 3.94 Torr.

resolving power values. Figure 3A shows the scaling of resolving power for Agilent tune mix compounds (m/z 322 - 1522) in different drift gases. The experiments were performed using direct infusion of the tune mix solution and signal averaging over 1 min. For all experiments the drift tube pressure was maintained at 3.94 Torr and the pressure in the trap funnel was maintained lower than the drift tube pressure. The drift field was maintained at 8.3 V/cm and 19.9 V/cm for helium and sulfur hexafluoride, respectively. For all other gases the drift field was maintained at 17.3 V/cm. The data shown in Figure 3B were acquired under the same conditions except the drift field for sulfur hexafluoride was maintained at 17.3 V/cm. Resolving power calculations were performed using the first isotope peak for each ion to avoid the space charge related effects. The highest resolving power (62.0) was obtained for the m/z 322 ion using nitrous oxide drift gas and the lowest resolving power (41.2) was obtained for the m/z 322 ion using helium drift gas due to under sampling of the drift peak. The temporal separation between data points across a given drift peak is ~ 120 μ s for m/z 1700 mass range. This is a fixed parameter that depends on the TOF pulser frequency in the mass range selected. The higher resolving powers (62.0, 60.7, 58.9 and 58.1 for N_2O , CO_2 , SF_6 , and N_2 , respectively) observed for the m/z 322 ion can be attributed to its relatively small and compact structure. On average nitrogen, nitrous oxide and carbon dioxide showed similar resolving powers for all ions studied. Sulfur hexafluoride showed lower resolving powers for most of the ions except m/z 322 ion; hypothetically this can be attributed to higher ion scattering due to larger CCS of the SF_6 . Smaller mass ions show reduced resolving power due to under sampling in helium drift gas. Figure 3B shows the separation of melezitose and raffinose mixture using different drift gases. This experiment was run under the same instrumental conditions as the data for Figure 3A. Here the degree of peak separation was assessed by calculating the chromatographic resolution for melezitose and raffinose peaks. For a chromatographic system, the degree of peak separation (R_s) is calculated using equation (10)

$$R_s = \frac{1.18(t_{D2} - t_{D1})}{w_{h1} + w_{h2}} \quad (10)$$

where t_{D1} , t_{D2} , w_{h1} , and w_{h2} are drift time of peak 1 and peak 2 and FWHM of peak 1 and peak 2, respectively. Here, peak 2 has the longer drift time compared to peak 1. The highest peak resolution was observed for nitrogen (1.31) while the lowest peak resolution was observed for sulfur hexafluoride (0.65). The peak resolutions for helium, carbon dioxide and nitrous oxide are 1.30, 1.00 and 1.01, respectively. The resolving power observed for melezitose and raffinose peaks were slightly different to the resolving power values obtained for the similar m/z 622 ion in the tune mix for the different drift gases. Nitrogen drift gas provided the best resolving power for melezitose and raffinose peaks (62.3 and 62.8, respectively), while sulfur hexafluoride provided the lowest resolving power 40.4 and 39.6, respectively. The peak resolution and resolving power values for melezitose and raffinose using sulfur hexafluoride were calculated using Gaussian fits to the peak data because the two peaks were only partially separated. The

resolving power values for melezitose and raffinose peaks in helium, carbon dioxide and nitrous oxide are 44.9, 45.8; 57.8, 58.3; and 60.8, 58.2, respectively. The lower resolving power observed for helium is due to the under sampling of the drift peaks. Generally the degree of separation for these two structural isomers decreased with increasing polarizability of the drift gas used. Drift gases with small collision cross sections and with low polarizability are favorable for the mobility separation of chemically similar compounds with slightly different structures. Since the separation of two compounds in a drift tube is a function of both momentum transfer collision cross section and long range and short range ion-neutral interactions, for the separation of chemically similar compounds, the collision cross section component of this interaction should dominate the ion-neutral induce dipole interactions.

Pesticide CCS Trends

The comprehensive pesticide mixture was analyzed using the LC-IM-MS method to generate CCS data bases for the different drift gases and to compare the relative CCS shifts. As noted previously, the drift gases were selected due to their polarizability characteristics. Helium was the least polarizable gas (0.20×10^{-24} cm^3) and SF_6 had the highest polarizability (6.54×10^{-24} cm^3).^{18,39} Nitrogen, carbon dioxide and nitrous oxide have 1.74×10^{-24} , 2.91×10^{-24} and 3.03×10^{-24} cm^3 polarizabilities, respectively.¹⁸ In addition to its polarizability, N_2O also contains a permanent dipole moment of 0.167 Debye. As a part of the data analysis process, features in the Q-TOF data was analyzed using the Find-by-Formula algorithm within MassHunter Qualitative Analysis. The Find-by-Formula generated a peak list with identified pesticides and the corresponding retention times. These data were used in a subsequent step to align peaks from the LC-IM-MS data sets. For peak picking and identification, the retention time window was ± 0.2 min. and the mass window was 25 ppm. All experiments were run in triplicate and data with %RSD values for the CCS measurements greater than 0.5 were rejected. Nitrogen gas experiments had the highest number of identifications. For helium, 406 total peaks were identified among all of the charge carrier species - 175 proton, 158 sodium, 60 potassium and 13 ammonium. For nitrogen drift gas experiments, a total of 561 pesticides were identified - 235 proton, 218 sodium, 93 potassium and 15 ammonium. Carbon dioxide experiments generated total of 265 pesticide identifications - 118 proton, 102 sodium, 38 potassium and 7 ammonium. For nitrous oxide experiments, total of 310 pesticides were identified - 147 proton, 113 sodium, 42 potassium and 8 ammonium. The sulfur hexafluoride drift gas experiments generated the fewest identifications at 255 pesticide identification - 132 proton, 106 sodium, 12 potassium and 5 ammonium.

The signal intensities for the SF_6 experiments were a factor of 5-7 lower than the nitrogen based experiment. The helium gas experiments gave the highest signal intensity, about factor of 2 higher than the nitrogen based experiments.

Figure 4 shows the CCS versus m/z plots for the different drift gases. These scatter plots can be fitted to power law equations with good agreement. Power law equations can describe the variation in volume or collision cross section with the increased mass of a molecule.^{3,36} All of the measured CCS values for different gases were located in a relatively narrow area of the plot indicating there were no significant CCS shifts based on the drift gas used. However, minor CCS shifts are readily observable with more polarizable drift gases. Based on the power law fits obtained for different adducts, the coefficients show similar magnitude between adducts for the same gas. The differing coefficients between helium and nitrogen indicates that polarizability of the drift gas affects the CCS calculations. The coefficients for the CO₂ and N₂O are on the same order of magnitude, indicating the similar nature of the induced-dipole interactions between these two gases and the analyte ions, except for the ammonium adduct in N₂O gas. Figure 5 shows the correlation plots for helium based CCS values and the CCS values based on other gases. Similar to the results shown in Figure 4, the scattering of the data points around the regression line is relatively tight. However, the slope and intercept for each of the adducted pesticide groups in the drift gases are different. The slope and intercept for all adducts in CO₂ and N₂O have similar magnitudes, again indicating the similar interactions between the drift gas and the analyte ions. The six ammonium adduct ions that are common between the helium and N₂O based experiments show a wide scattering in the correlation plot (Figure 5C). These ions did not result a linear regression line as expected and this may indicate selective CCS shifting when using N₂O for ammonium adduct separation. This

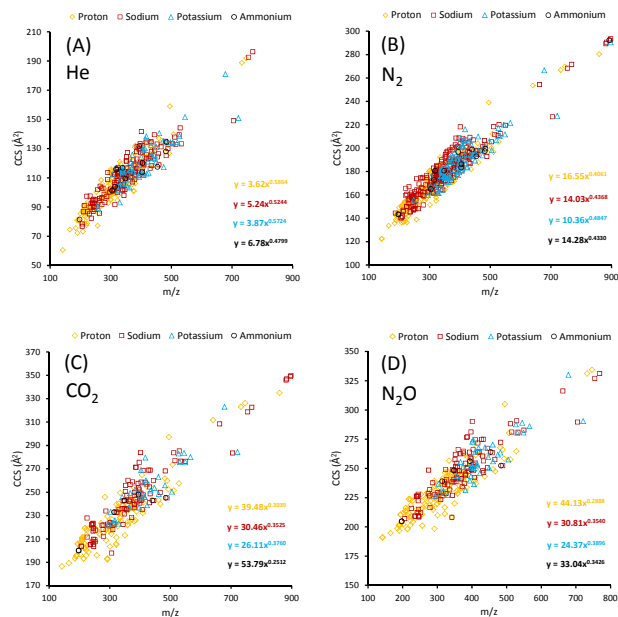


Figure 4. CCS versus m/z plots for pesticides in different drift gases. Plots (A), (B), (C), and (D) correspond to helium, nitrogen, carbon dioxide and nitrous oxide drift gases, respectively. For each plot, ions containing protons, sodium, potassium and ammonium adducts as charge carriers were included. All ions included in these plots are +1 charge state. Data for each cation type is fitted to a power regression line and the equations are given on the plots. Pesticide LC experiments were run at 8.3 V/cm for helium and 17.3 V/cm for all the other gases.

observation needs further investigation with a larger sample population.

There were 389 ions common between the helium and nitrogen (He-N₂) experiments. Between He-CO₂, He-N₂O and He-SF₆ experiments, there were 182, 216, and 219 common ions, respectively. The average CCS for the helium experiments was $111.3 \pm 18.2 \text{ \AA}^2$. The average CCS for the CO₂ experiments was $236.1 \pm 26.9 \text{ \AA}^2$ and for N₂O and SF₆, the average CCS values were 242.5 ± 25.5 and $288.6 \pm 21.9 \text{ \AA}^2$, respectively. The CCS values on average for the pesticides in nitrogen gas increased by a factor of 1.60 when compared to the helium based values. This value is increased by a factor of 2.10, 2.15, and 2.58 for CO₂, N₂O and SF₆ gases respectively. Although the magnitude of the CCS values are increasing with larger and more polarizable gases, the data did not indicate significant improvement in overall peak capacity and the total separation space. Figure 6 provides information about the scattering of the data points around the regression lines from the Figure 5 correlation plots. Figure 6A shows data from Figure 5A and the average CCS space is $\pm 2 \text{ \AA}^2$ for protonated ions. For other adducts, the average CCS spaces are ± 2.2 , ± 2.6 , and $\pm 7.3 \text{ \AA}^2$ for the sodium, potassium and ammonium species, respectively. Figure 6B shows data for helium and CO₂ experiments. The average CCS spread around the regression lines are ± 5.9 , ± 4.8 , ± 4.3 , and $\pm 5.3 \text{ \AA}^2$ for proton, sodium, potassium and ammonium species, respectively. Figures 6C and D are for N₂O and SF₆ experiments and correlation plots compared to helium experiments. The average CCS spreads for Figure 6C are ± 4.3 , ± 4.5 , and $\pm 4.3 \text{ \AA}^2$ for proton, sodium and potassium species, respectively. Since there were no usable regression lines for the ammonium adduct data

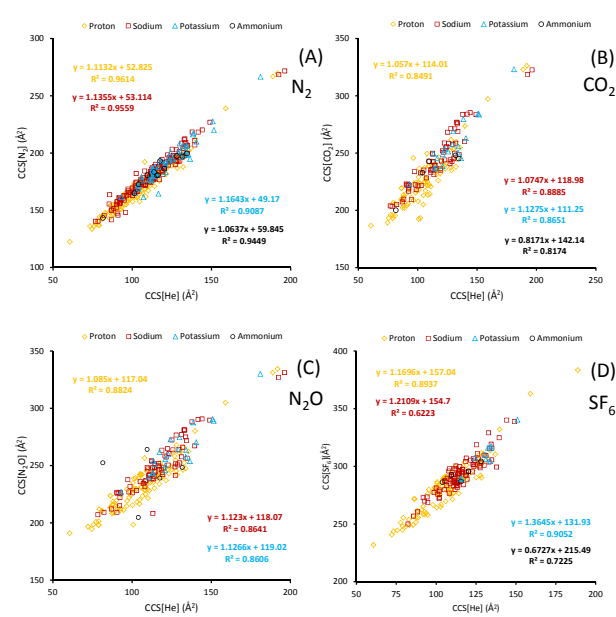


Figure 5. Correlation plots for CCS values between nitrogen, carbon dioxide, nitrous oxide, and sulfur hexafluoride versus helium drift gas for pesticides. The plots include ions containing protons, sodium, potassium and ammonium adducts. Linear regression results for each adduct type are shown. Based on the R² values, the nitrogen versus helium plot (A) provided the best correlation and both carbon dioxide (B) and nitrous oxide (C) had similar correlations with helium CCS values. A much lower correlation was obtained with sulfur hexafluoride versus helium (D).

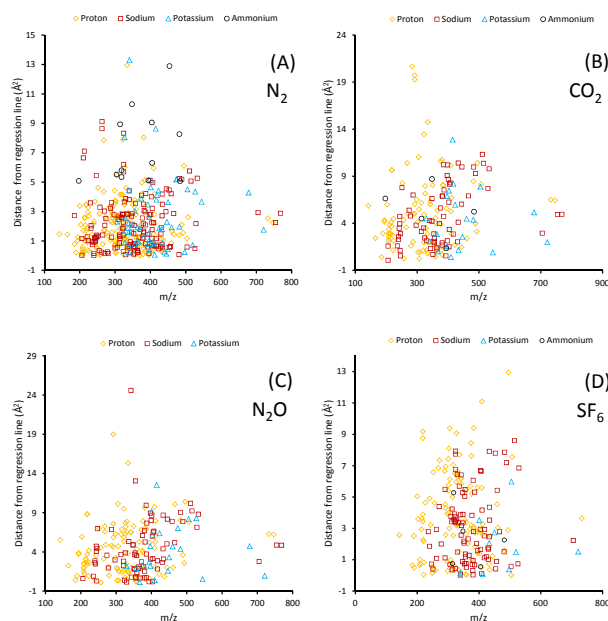


Figure 6. The distance between each CCS data point in the Figure 5 plots and the regression line against the mass of corresponding ion are plotted. These graphs show the magnitude of the CCS distribution in the correlation plots between helium and other gases. (A) Corresponds to the data in Figure 5(A). (B), (C), and (D) correspond to the data in Figures 5(B), 5(C), and 5(D), respectively. Ions with different charge carriers are depicted using different symbols and colors.

(Figure 5C), the CCS spread was not included in Figure 6C for N_2O . The average CCS spreads for Figure 6C are ± 3.8 , ± 3.8 , ± 1.8 , and $\pm 2.3 \text{ \AA}^2$ for proton, sodium, potassium and ammonium species, respectively, in SF_6 . The results for the pesticide experiments show that the use of polarizable gases do not necessarily improve separation efficiency for all the compounds in a complex sample and peak capacity for the overall analysis. Further investigations are needed to understand the use of polar gases for targeted separation of chemically different compounds.

Table 1 lists CCS values for several proton and sodium adducted isomeric pesticides in helium, nitrogen, carbon dioxide and nitrous oxide drift gases. In general, a slight improvement in separation is noted for the isomeric species when there is a slightly larger difference between the measured CCS values. However, it is important to note that the increased difference between the measured CCS values may not have resulted from an increased peak resolution, but may have been due to the overall larger CCS values in more polarizable and larger drift gases.

There are few notable trends observed from the separation and CCS values in this study. For example, the use of different charge carriers other than protons may improve separation in conjunction with more polarizable gases, as evident by the larger CCS difference for azaconazole with a sodium adduct. For example, the protonated species for azaconazole in N_2 drift gas produced CCS values of 163.7 and 164.6 \AA^2 for isomer 1 and isomer 2, respectively, while the sodiated species produced values of 166.2 and 169.4 \AA^2 . However, in general the isomers included in this table do not necessarily show improved

separation with more polarizable drift gases. The lack of improved separation suggest that these isomers have very similar structures and surface charge localizations. Campuzano and co-workers have shown that more polarizable drift gases can be used to selectively separate isomers with significantly different surface charge distributions.¹⁸ The CCS values in Table 1 do show a consistent increase with the size and polarizability of the drift gas.

Conclusions

In this study, an ion mobility Q-TOF mass spectrometer with the capability to utilize alternate drift gases was used to study the feasibility of employing polarizable drift gases for complex sample analyses. Recent developments in hybrid ion mobility mass spectrometry instrumentation and the commercial availability of various instruments from different vendors has opened the door for the wider acceptance and regular use of this technique for complex and challenging applications and problem solving. The instrument used in this study is capable of separating complex mixtures using the ion mobility technology and detecting those gas-phase separated compounds with high accuracy, throughput⁴⁰ and sensitivity. The low pressure drift tube and low electric field operation utilized is uniquely suited for high throughput applications and structural analysis. The CCS values generated using the drift time information for each ion can be used as a unique compound identifier in combination with retention time and accurate mass measurements. In this study, retention time and accurate mass was used to identify the compounds in addition to the isotopic pattern distribution for each analyte ion.

The pesticide standards studied in this application were relatively complex and contained many isobaric and isomeric compounds that may or may not be separated by high performance liquid chromatographic methods. In such cases, additional separation that can be achieved before mass analysis provide a significant benefit in identifying and characterizing compounds in complex samples.

The momentum transfer kinetic theory explains that the CCS values obtained in an ion mobility experiment is a function of the long range induced dipole interactions as well as short range repulsive interactions between analyte ions and drift gas molecules. In this study, employing different drift gases to separate two structural isomers showed that highly polarizable gases did not necessarily improve the separation of the chemically similar ions. This can be explain by the strong interaction between the analyte ions and the drift gas molecules. This interaction essentially reduces the separation achieved purely due to structural differences between the analyte ions. The data for the pesticide analysis indicate that the use of highly polarizable gases do not improve the selectivity and separation for all the compounds globally. Instead this technique may be utilized under favourable conditions to selectively separate targeted compounds with different chemical and surface electronic charge distributions.

Table 1. CCS values for several isomeric pesticides in different drift gases.

| Pesticide Compound Name | Formula | Mass (Da) | Retention Time (min) | He-CCS (\AA^2) | | N_2 -CCS (\AA^2) | | CO_2 -CCS (\AA^2) | | N_2O -CCS (\AA^2) | |
|----------------------------|---|-----------|-------------------------|---------------------------|--------------------|--------------------------------------|--------------------|---------------------------------------|--------------------|--|--------------------|
| | | | | [H ⁺] | [Na ⁺] | [H ⁺] | [Na ⁺] | [H ⁺] | [Na ⁺] | [H ⁺] | [Na ⁺] |
| Acephate | $\text{C}_4\text{H}_{10}\text{NO}_3\text{PS}$ | 183.0119 | 2.29 | | 76.9 | | 140.4 | | 203.9 | | |
| | | | 2.61 | | 78.4 | | 140.4 | | 203.4 | | 207.0 |
| Aminocarb | $\text{C}_{11}\text{H}_{16}\text{N}_2\text{O}_2$ | 208.1212 | 2.87 | 88.0 | | 151.1 | | 211.3 | | 216.2 | |
| | | | 2.97 | 88.0 | | 151.1 | | 211.3 | | 216.3 | |
| Azaconazole | $\text{C}_{12}\text{H}_{11}\text{Cl}_2\text{N}_3\text{O}_2$ | 299.0228 | 9.16 | 94.9 | | 163.7 | 166.2 | | | | |
| | | | 10.05 | 95.4 | | 164.6 | 169.4 | | | | |
| Bromuconazole | $\text{C}_{13}\text{H}_{12}\text{BrCl}_2\text{N}_3\text{O}$ | 374.9541 | 12.18 | 100.7 | | 171.2 | | | | | |
| | | | 13.26 | 101.3 | | 173.0 | | 236.5 | | 238.6 | |
| Chlorfenvinphos | $\text{C}_{12}\text{H}_{14}\text{Cl}_3\text{O}_4\text{P}$ | 357.9695 | 13.89 | 107.7 | 114.2 | 168.5 | 180.3 | | | | |
| | | | 14.26 | 108.5 | 114.7 | 168.8 | 181.0 | 221.9 | 239.3 | 228.4 | 244.6 |
| Epoxiconazole | $\text{C}_{17}\text{H}_{13}\text{ClFN}_3\text{O}$ | 329.0731 | 11.95 | 104.8 | | 173.1 | | | | | |
| | | | 12.80 | 106.4 | | 175.3 | 178.9 | | | 242.2 | 247.1 |
| Flutriafol | $\text{C}_{16}\text{H}_{13}\text{F}_2\text{N}_3\text{O}$ | 301.1027 | 8.57 | 97.9 | 108.3 | 165.1 | 182.1 | | | | |
| | | | 9.72 | 98.8 | 102.5 | 166.8 | 172.7 | 224.5 | 232.8 | | |
| Iaconazole | $\text{C}_{18}\text{H}_{24}\text{ClN}_3\text{O}$ | 333.1608 | 14.75 | 106.9 | 111.3 | 172.6 | 178.6 | 228.2 | 235.6 | 235.1 | 242.0 |
| | | | 15.00 | 107.0 | 111.2 | 172.9 | 178.4 | 228.3 | 235.0 | 235.3 | 241.7 |
| Metconazole | $\text{C}_{17}\text{H}_{22}\text{ClN}_3\text{O}$ | 319.1451 | 12.10 | 102.2 | | 169.3 | | | | | |
| | | | 14.12 | 101.8 | 105.6 | 168.3 | 174.2 | 223.3 | | 229.8 | |
| Methacrifos | $\text{C}_7\text{H}_{13}\text{O}_5\text{PS}$ | 240.0221 | 9.36 | | 85.8 | | 148.2 | | | | |
| | | | 10.42 | | 95.9 | | 163.6 | | | | |
| Omethoate | $\text{C}_5\text{H}_{12}\text{NO}_4\text{PS}$ | 213.0225 | 2.79 | 78.9 | 82.3 | 136.8 | 145.5 | 193.2 | 205.1 | 198.1 | 209.2 |
| | | | 2.93 | 78.9 | | 136.8 | | 193.2 | | 198.1 | |
| Propiconazole | $\text{C}_{15}\text{H}_{17}\text{Cl}_2\text{N}_3\text{O}_2$ | 341.0698 | 13.81 | 109.4 | 113.0 | 178.8 | 181.0 | 238.4 | 242.6 | 245.3 | 248.1 |
| | | | 13.88 | 109.4 | 113.1 | 178.8 | 181.0 | 238.9 | 242.2 | 245.3 | 247.9 |
| Pymetrozine | $\text{C}_{10}\text{H}_{11}\text{N}_5\text{O}$ | 217.0964 | 2.65 | 86.3 | 92.7 | 154.1 | 158.2 | 219.3 | 222.2 | 223.7 | 226.1 |
| | | | 2.98 | 86.3 | 92.5 | 154.1 | 158.2 | 219.3 | 222.0 | 223.7 | 226.2 |
| Tebuconazole | $\text{C}_{16}\text{H}_{22}\text{ClN}_3\text{O}$ | 307.1451 | 11.55 | 101.4 | | 167.6 | 174.2 | | | | |
| | | | 13.64 | 100.7 | | 166.1 | 172.4 | 221.8 | 235.2 | 228.5 | 235.9 |
| Triticonazole | $\text{C}_{17}\text{H}_{20}\text{ClN}_3\text{O}$ | 317.1295 | 10.96 | 107.4 | 114.0 | 178.6 | 188.3 | | | | |
| | | | 12.64 | | 114.8 | | 190.1 | | | | |

Acknowledgements

The authors would like to acknowledge Alex Mordehai, Mark Werlich, Tom Knotts, Layne Howard, Chris Klein, Bill Frazer, Yevgeny Kaplun and Bill Barry for their contribution in the IM-QTOF instrument development, and Gregor Overney, Bruce Wang, Sandra Tang and Huy Bui for their support in instrument control software development.

Notes and References

- E. W. McDaniel, *Collision phenomena in ionized gases*, Wiley, New York, 1964.
- F. W. Karasek, *Anal. Chem.*, 1974, **46**, 710A-720A.
- H. E. Revercomb and E. A. Mason, *Analytical Chemistry*, 1975, **47**, 970-983.
- S. J. Valentine, X. Liu, M. D. Plasencia, A. E. Hilderbrand, R. T. Kurulugama, S. L. Koeniger and D. E. Clemmer, *Expert Rev. Proteomics*, 2005, **2**, 553-565.
- D. E. Clemmer and M. F. Jarrold, *J. Mass Spectrom.*, 1997, **32**, 577-592.
- M. T. Bowers, *Int. J. Mass Spectrom.*, 2015, **377**, 625-645.
- P. Dugourd, R. R. Hudgins, D. E. Clemmer and M. F. Jarrold, *Rev. Sci. Instrum.*, 1997, **68**, 1122-1129.
- S. J. Valentine, M. Kulchania, C. A. Srebalus Barnes and D. E. Clemmer, *Int. J. Mass Spectrom.*, 2001, **212**, 97-109.
- T. Wyttenbach, G. von Helden, J. J. Batka, D. Carlat and M. T. Bowers, *J. Am. Soc. Mass Spectrom.*, 1997, **8**, 275-282.
- M. F. Mesleh, J. M. Hunter, A. A. Shvartsburg, G. C. Schatz and M. F. Jarrold, *J. Phys. Chem.*, 1996, **100**, 16082-16086.
- A. A. Shvartsburg and M. F. Jarrold, *Chem. Phys. Lett.*, 1996, **261**, 86-91.
- N. E. Bradbury, *Phys. Rev.*, 1932, **40**, 508-523.
- H. H. Hill, W. F. Siems, R. H. St. Louis and D. G. McMinn, *Anal. Chem.*, 1990, **62**, 1201A-1209A.
- S. A. Shaffer, D. C. Prior, G. A. Anderson, H. R. Udseth and R. D. Smith, *Anal. Chem.*, 1998, **70**, 4111-4119.
- Y. Ibrahim, M. E. Belov, A. V. Tolmachev, D. C. Prior and R. D. Smith, *Anal. Chem.*, 2007, **79**, 7845-7852.
- J. A. McLean, B. T. Ruotolo, K. J. Gillig and D. H. Russell, *Int. J. Mass Spectrom.*, 2005, **240**, 301-315.
- S. Rokushika, H. Hatano and H. H. Hill, *Anal. Chem.*, 1986, **58**, 361-365.
- P. M. Lalli, Y. E. Corilo, M. Fasciotti, M. F. Riccio, G. F. de Sa, R. J. Daroda, G. H. M. F. Souza, M. McCullagh, M. D. Bartberger, M. N. Eberlin and I. D. G. Campuzano, *J. Mass Spectrom.*, 2013, **48**, 989-997.
- M. D. Howdle, C. Eckers, A. M. F. Laures and C. S. Creaser, *Int. J. Mass Spectrom.*, 2010, **298**, 72-77.
- B. T. Ruotolo, J. A. McLean, K. J. Gillig and D. H. Russell, *J. Mass Spectrom.*, 2004, **39**, 361-367.
- C. Larriba-Andaluz, J. Fernandez-Garcia, M. A. Ewing, C. J. Hogan Jr., D. E. Clemmer, *Phys. Chem. Chem. Phys.*, 2015, **17**(22), 15019-15029.
- C. Larriba, C. J. Hogan Jr., *J. Phys. Chem. A*, 2013, **117**, 3887-3901.

- 1
2
3
4
5
6
7
8
9
10
11
12
13
14
15
16
17
18
19
20
21
22
23
24
25
26
27
28
29
30
31
32
33
34
35
36
37
38
39
40
41
42
43
44
45
46
47
48
49
50
51
52
53
54
55
56
57
58
59
60
- 23 H. Ouyang, C. Larriba-Andaluz, D. R. Oberreit, C. J. Hogan Jr., *J. Am. Soc. Mass. Spectrom.*, 2013, **24**, 1833-1847.
- 24 L. M. Matz, L. W. Beegle, I. Kanik and H. H. Hill, *J. Am. Soc. Mass Spectrom.*, 2002, **13**, 300-307.
- 25 S. L. Koeniger, S. I. Merenbloom, S. J. Valentine, M. F. Jarrold, H. R. Udseth, R. D. Smith, D. E. Clemmer, *Anal. Chem.*, 2006, **78**, 4161-4174.
- 26 M. D. Howdle, C. Eckers, A. M.-F. Laures, C. S. Creaser, *J. Am. Soc. Mass Spectrom.*, 2009, **20**, 1-9.
- 27 B. C. Bohrer and D. E. Clemmer, *Anal. Chem.*, 2011, **83**, 5377-5385.
- 28 P. Dwivedi, C. Wu, L. M. Matz, B. H. Clowers, W. F. Siems and H. H. Hill, *Anal. Chem.*, 2006, **78**, 8200-8206.
- 29 E. A. Mason and E. W. McDaniel, *Transport Properties of Ions in Gases*, Wiley, New York, 1988.
- 30 M. F. Bush, I. D. G. Campuzano, C. V. Robinson, *Anal. Chem.*, 2012, **84**, 7124-7130.
- 31 I. Campuzano, M. F. Bush, C. V. Robinson, C. Beaumont, K. Richardson, H. Kim, H. I. Kim, *Anal. Chem.*, 2012, **84**, 1026-1033.
- 32 A. Mordehai, R. Kurulugama, E. Darland, G. Stafford and J. Fjeldsted, *Proceedings of the ASMS Conference*, 2015, MP 126, St. Louis, MO.
- 33 J. R. Enders, J. A. McLean, *Chirality*, 2009, **21**, E253-E264.
- 34 A. Bondi, *J. Phys. Chem.*, 1964, **68**, 441-451.
- 35 H. Kim, H. I. Kim, P. V. Johnson, L. W. Beegle, J. L. Beauchamp, W. A. Goddard, I. Kanik, *Anal. Chem.*, 2008, **80**, 1928-1936.
- 36 J. C. May, C. R. Goodwin, N. M. Lareau, K. L. Leaptrot, C. B. Morris, R. T. Kurulugama, A. Mordehai, C. Klein, W. Barry, E. Darland, G. Overney, K. Imatani, G. C. Stafford, J. C. Fjeldsted and J. A. McLean, *Anal. Chem.*, 2014, **86**, 2107-2116.
- 37 A. V. Tolmachev, B. H. Clowers, M. E. Belov and R. D. Smith, *Anal. Chem.*, 2009, **81**, 4778-4787.
- 38 T. Wyttenbach, N. A. Pierson, D. E. Clemmer and M. T. Bowers, *Annu. Rev. Phys. Chem.*, 2014, **65**, 175-196.
- 39 L. W. Beegle, I. Kanik, L. Matz, H. H. Hill, *Int. J. Mass Spectrom.*, 2002, **216**, 257-268.
- 40 J. M. Santos, R. de S. Galaverna, M. A. Pudenzi, E. M. Schmidt, N. L. Sanders, R. T. Kurulugama, A. Mordehai, G. C. Stafford, A. Wisniewski Jr. and M. N. Eberlin, *Anal. Methods*, 2015 **7**, 4450-4463.